Permutations of the transverse momentum dependent effective valence-band potential for layered heterostructures. Pseudomorphic strain effects.

L. Diago-Cisneros[1,2] J. J. Flores-Godoy[1] A. Mendoza-Álvarez[1], and G. Fernández-Anaya[1]

E-mail: ldiago@fisica.uh.cu

[1]Departamento de Física y Matemáticas, Universidad Iberoamericana, México D. F., C. P. 01219, México.

[2] Facultad de Física, Universidad de La Habana C. P. 10400, Cuba.

Abstract. The evolution of transverse-momentum-dependent effective band offset (V_{eff}) profile for heavy (hh)- and light-holes (lh), is detailed studied. Several new features in the metamorphosis of the standardized fixed-height V_{eff} profile for holes, in the presence of gradually increasing valence-band mixing and pseudomorphic strain, are presented. In some $III-V$ unstrained semiconducting layered heterostructures a fixed-height potential, is not longer valid for lh. Indeed, we found –as predicted for electrons–, permutations of the V_{eff} character for lh, that resemble a "*keyboard*", together with bandgap changes, whenever the valence-band mixing varies from low to large intensity. Strain is able to diminish the *keyboard* effect on V_{eff}, and also makes it emerge or vanish occasionally. We found that multiband-mixing effects and stress induced events, are competitors mechanisms that can not be universally neglected by assuming a fixed-height rectangular spatial distribution for fixed-character potential energy, as a reliable test-run input for heterostructures. Prior to the present report, neither direct transport-domain measurements, nor theoretical calculations addressed to these V_{eff} evolutions and permutations, has been reported for holes, as far as we know. Our results may be of relevance for promising heterostructure's design guided by valence-band structure modeling to enhance the hole mobility in $III-V$ materials.

PACS numbers: 71.70.Ej, 72.25.Dc, 73.21.Hb, 73.23.Ad

1. Sinopsis of Fundamentals and Motivation

For many actual practical solutions and technological applications, due to the impressive development of low-dimensional electronic and optoelectronic devices, it is drastically important to include the valence-band mixing [1], *i.e.* the degree of freedom transverse to the main transport direction, whenever the holes are involved. This phenomenology, early quoted by Wessel and Altarelli in resonant tunneling [2], has been lately pointed up for real-life technological devices [1]. If the electronic transport through these systems, engage both electrons and holes, the low-dimensional device response depends on the slower-heavier charge-carrier's motion through specific potential regions [3]. It is unavoidable to recognize that in the specialized literature there is plenty of reports studying several physical phenomena derived from hole mixing effects and strain, *via* standard existing methods. Some authors had managed to determine optimal situation in a resonant tunneling of holes under internal strains, disregarding scattering effects and assuming a spatial symmetry for a constant potential [4]. A fundamental study on valence-band mixing in first-principles, established a non-linear response for a pseudo-potential in series of the atomic distribution function [5]. Valence-band mixing and/or strain had been extensively studied over the past few decades in several nanostructures ranging from quantum wells [4, 6, 7, 8], to quantum wires [9, 10] and to quantum dots [11]. However, just a few reports are available, concerning the very evolution itself of the effective potential due to several causes, as a central topic of research. We underline in the present paper the focus not on valence-band mixing and strain effects problem in general, but rather on the particular metamorphosis of the effective potential while manipulating both effects. We hope to make some progress in understanding the underlaying physics as well as determine whether or not the valence-band mixing and strain are competitors mechanism in the evolution of the effective potential.

Earliest striking elucidations due to Milanović and Tjapkin for electrons,[12] and recalled much later by Pérez-Álvarez and García-Moliner for a fully unspecific multiband theoretical case,[13] are fundamental cornerstones in this concern. The metamorphosis of the effective *band offset* potential V_{eff}, "felt" by charge carriers depending on the transverse momentum value, is so far, the better way to graphically mimic, the phenomenon of the in-plane dependence of the effective mass, also refereed as the valence-band mixing for holes. In few words, a hole band mixing is crucial for bulk and low-dimensional confined systems possessing quantal heterogeneity, a question soon to be discussed in this paper, inspired in a similar scenario, as was done before for a single-band-electron problem [12]. Particularities of the appealing evolution features of V_{eff} for holes, in the presence of gradually increasing valence-band mixing and strain, could be of interest for condensed-matter physicists, working in the area of quantum transport for multiband-multichannel models. While previous studies in quantum systems have added substantial contributions to the elucidation of the valence-subband structure [1], and the influence of the hole mixing on it [5, 12, 13], there remain some aspects which

do not appear to have received yet sufficient attention and/or because of their interest deserve further clarification. This is essentially the case of the strain influence together with carriers' transverse motion connection with the V_{eff} they interact with, which are the main porpoises under investigation here. We assume the last, widely understood as crucial for charge and spin carriers' quantum transport calculations through standard quantum barrier(QB) – quantum well(QW) layered systems.

On general grounds, V_{eff} is given by the difference for $3D$ band edge levels as long as the transverse momentum (κ_{T}) values are negligible.[13] For finite κ_{T}, this assertion is no longer valid and the mixing effects reveal. The mechanism responsible for this behavior, is the increment of the κ_{T}-quadratic proportional term, yielding even to invert the roles of QW and QB [12, 13]. Some authors had declared a shift upward in energy, of the bound states in the effective potential well as the transverse wave vector increases [14]. By letting grow κ_{T}, were found the valence-band mixing effects to arise and V_{eff} to change [15]. They conclude a larger reduction for V_{eff} as a function of κ_{T}, for light holes (lh) respect to that for heavy holes (hh) [15]. These former works [5, 12, 13, 14, 15], were motivating enough and put us on an effort to try a more comprehensive vision, of how V_{eff} evolves spatially with κ_{T} and strain, for hh and lh. This paper is devoted to demonstrate, the feasibility of the V_{eff} profile evolution, QB-QW permutations, and bandgap changes, as a reliable follow-up tools for finding the response of a layered semiconductor system —with spatial-dependent effective mass—, on travelling holes throughout it, by tuning the valence-band mixing and including stress effects.

Built-in elastic strained layered heterostructures, has been remarkably used in the last decade, for development of light-emitting diodes, lasers, solar cells and photodetectors.[16] Besides, internal strain may results into a considerably modification of the electronic structure of both electrons and holes, thereby altering the response of strained systems respect to nominal behavior of strain-free designs.[16] We get motivated about the probable existence of a competitor mechanism able to diminish the effects of valence-band mixing on V_{eff}, or wipe them out occasionally. Thus, owing to the need to account for strain in the present study, we additionally suppose the heterostructure sandwiched into an arbitrary configuration of pseudomorphically strained sequence of QW-acting and QB-acting binary(ternary) allows, due technological interest in that configuration. Whenever on layer-by-layer deposition, the epitaxially grown layer's lattice parameter matches that of the substrate in the in-plane direction –without collateral dislocations or vacancies–, the process is referred as pseudomorphic [see Fig. 1(b)].[17] The last is widely chosen for most day-to-day applications, designed on a write-read platform, such as sound/image players and data-manipulating devices.

The outline for this paper is the following: Section 2 presents briefly the theoretical framework to quote valence-band V_{eff} for both unstressed and stressed systems. Graphical simulations on V_{eff} evolution, are exposed in Section 3. In that section, we exercise and discuss highly specialized $III-V$ semiconductor binary(ternary)-compound cases, that support the main contribution of the present study and suggest possible applications. Section 4, contains some conclusions.

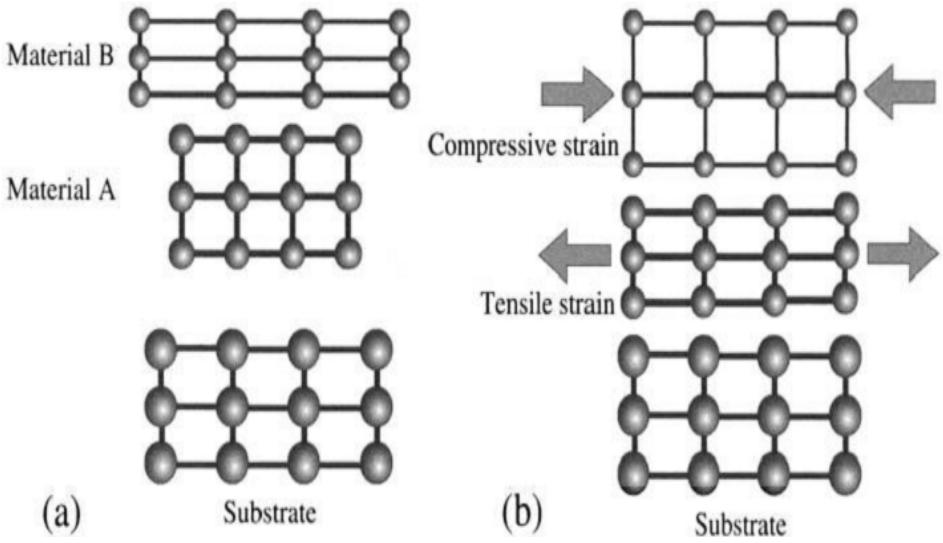

Figure 1. Panel (a) shows the stress-free bulk materials, with lattice parameter $a_l < a_s$ smaller (*GaAsP*), and larger $a_l > a_s$ (*InGaAs*) than that of the substrate.[18] Panel (b) illustrates a schematic representation of a pseudomorphic grown process for a layered heterostructure.[17] The material *GaAsP* is under a tensile strain, while the material (*InGaAs*) is under compressive strain, as they both are forced to conform the buffer's lattice constant a_s of a suitable semiconductor wafer.

2. Calculation of the effective potential

Commonly, a wide class of solid-state physics problems, related to electronic and transport properties, demands the solution of multiband-coupled differential system of equations, widely known as Sturm-Liouville matrix generalized boundary problem [13]:

$$\frac{d}{dz}\left[\boldsymbol{B}(z)\frac{d\boldsymbol{F}(z)}{dz}+\boldsymbol{P}(z)\boldsymbol{F}(z)\right]+\boldsymbol{Y}(z)\frac{d\boldsymbol{F}(z)}{dz}+\boldsymbol{W}(z)\boldsymbol{F}(z)=\boldsymbol{O}_{\mathrm{N}}, \tag{1}$$

where $\boldsymbol{B}(z)$ and $\boldsymbol{W}(z)$ are, in general, $(N\times N)$ Hermitian matrices and is fulfilled $\boldsymbol{Y}(z)=-\boldsymbol{P}^{\dagger}(z)$. In the absence of external fields, standard plane-wave solutions are assumed and it is straightforward to derive a non-linear algebraic problem

$$\boldsymbol{Q}(k_z)\boldsymbol{\Gamma}=\left\{k_z^2\boldsymbol{\mathcal{M}}+k_z\,\boldsymbol{\mathcal{C}}+\boldsymbol{\mathcal{K}}\right\}\boldsymbol{\Gamma}=\boldsymbol{O}_{\mathrm{N}}, \tag{2}$$

called as quadratic eigenvalue problem (QEP),[15] since $\boldsymbol{Q}(k_z)$ is a second-degree matrix polynomial on the z-component wavevector k_z. In the specific case of the well-known (4×4) Kohn-Lüttinger (KL) model Hamiltonian, the matrix coefficients of equation (2) bear a simple relation with those in (1) [15]:

$$\boldsymbol{\mathcal{M}}=-\boldsymbol{B},\ \ \boldsymbol{\mathcal{C}}=2i\boldsymbol{P}\ \text{ and }\ \boldsymbol{\mathcal{K}}=\boldsymbol{W}. \tag{3}$$

Then for (4×4) KL model, the matrix coefficients of (2) can be cast as :

$$\boldsymbol{\mathcal{M}}=\begin{pmatrix}-m_{hh}^{*} & 0 & 0 & 0\\ 0 & -m_{lh}^{*} & 0 & 0\\ 0 & 0 & -m_{h}^{*} & 0\\ 0 & 0 & 0 & -m_{hh}^{*}\end{pmatrix} \tag{4}$$

$$\boldsymbol{\mathcal{C}} = \begin{pmatrix} 0 & 0 & h_{13}+iH_{13} & 0 \\ 0 & 0 & 0 & -h_{13}-iH_{13} \\ h_{13}-iH_{13} & 0 & 0 & 0 \\ 0 & -h_{13}+iH_{13} & 0 & 0 \end{pmatrix} \tag{5}$$

$$\boldsymbol{\mathcal{K}} = \begin{pmatrix} a_1 & h_{12}+iH_{12} & 0 & 0 \\ h_{12}-iH_{12} & a_2 & 0 & 0 \\ 0 & 0 & a_2 & h_{12}+iH_{12} \\ 0 & 0 & h_{12}-iH_{12} & a_1 \end{pmatrix} \tag{6}$$

Here $m^*_{hh,lh}$ stands for the (hh,lh) effective mass, respectively. We briefly introduce some parameters and relevant quantities (in atomic units) of the KL model:

γ_i, with $i = 1, 2, 3$ [Lüttinger semi-empirical valence band parameters, typical for each semiconductor material].

$R = 13.60569172$ eV [Rhydberg constant],

$a_0 = 0.5405$ Å [Bohr radius],

V [Finite stationary barrier's height].

E [Energy of incident and uncoupled propagating modes],

k_x, k_y [Components of the transversal wavevector],

$A_{1,2} = a_0^2 R\,(\gamma_1 \pm \gamma_2)$,

$a_{1,2} = A_{1,2}\kappa_{\mathrm{T}}^2 + V(z) - E$,

$h_{12} = a_0^2 R\sqrt[2]{3}\gamma_2\left(k_y^2 - k_x^2\right)$,

$h_{13} = -a_0^2 R\sqrt[2]{3}\gamma_3 k_x$,

$H_{13} = a_0^2 R\sqrt[2]{3}\gamma_3 k_y$,

$H_{12} = a_0^2 R\sqrt[2]{3}2\gamma_3 k_x k_y$,

Bearing direct association to the original matrix dynamic equation, we exclusively focus to the case when $\boldsymbol{\mathcal{M}}$, $\boldsymbol{\mathcal{C}}$ and $\boldsymbol{\mathcal{K}}$ are constant-by-layer, hermitian; and $\boldsymbol{\mathcal{M}}$ is non-singular; therefore k_z are all different real (symmetric) or arises in conjugated pairs (k_z, k_z^*). Hereafter $\boldsymbol{O}_{\mathrm{N}}/\boldsymbol{I}_{\mathrm{N}}$, stand for $(N \times N)$ null/identity matrix. The QEP's solutions result in the eigenvalues k_{z_j} and the eigenvectors $\boldsymbol{\Gamma}_j$. As $\boldsymbol{Q}(k_z)$ is regular, eight finite-real or complex-conjugated pairs of eigenvalues are expected. Assuming a QEP method,[15, 19] it can be cast

$$\det\left[\boldsymbol{Q}(k_z)\right] = q_0 k_z^8 + q_1 k_z^6 + q_2 k_z^4 + q_3 k_z^2 + q_4, \tag{7}$$

which is an eighth-degree polynomial with only even power of k_z and real coefficients. The coefficients q_i are functions of the system's parameters, and $q_0 = \det \boldsymbol{\mathcal{M}}$ as expected.[19] In the specific case of the Kohn-Lüttinger (KL) model Hamiltonian,[15] q_i contain the Lüttinger semi-empirical valance-band parameters and the components of in-plane quasi-wave vector κ_{T}.

Based on our procedure [19], it is straightforward to follow whereas k_z is oscillatory or not by dealing with (7), and thereby the kind of V_{eff} the holes interplay with. We will refer to *root-locus-like* terminology from now on throughout the paper, whenever we proceed to invoke a complex-plane dependence, for the QEP (2) eigenvalues evolution as

the valence-band mixing parameter changes. To our knowledge, just few pure theoretical or numerical applications of the *root-locus-like* technique, particularly for the QEP scenario, had been previously addressed to explicitly describe several standard $III-V$ semiconductor compounds [19, 20]. We get motivated by the advantages of the *root-locus-like* technique in solid state physics [19, 20], and try to foretell here, new features of the particle-scatterer interaction in the presence of valence-band mixing and strain. For some high specialized zinc-blenda and wurtzite systems, current knowledge of the hole quantum transport mechanism, is far to be profound. The present theoretical contribution, claim to spread light on that issue. Mainly, we think here in readers that may be interested more on the way the effective valence-band offset metamorphosis with band mixing and strain, could influence on their day-to-day applications, rather than getting involved with the very details of the theoretical model itself, only. Owing to that concern, we propose a simple and comprehensive modelling procedure for V_{eff} to deal with, and a *gedanken*-like simulation for a passage of mixed holes throughout strained-free and strained layered heterostructures is exercised.

An effective potential, is found useful to describe valence-band mixing in the EFA.[5] In the case envisioned here, to determine the operator $\widehat{\boldsymbol{W}}_{\text{eff}}$ for the effective *band offset* potential, suffices to use the Kohn-Lüttinger (KL) model Hamiltonian,[15] considering the transverse quasi-momentum $\vec{\kappa}_{\text{T}} = k_x\widehat{e}_x + k_y\widehat{e}_y$, because this is the direction of the Brillouin Zone where is described the present KL Hamiltonian. We assume understood any modification of the selected Brillouin Zone direction, as a change in the model Hamiltonian to use. The system's quantal heterogeneity is considered along z axis, taken perpendicular to the heterostructure interfaces [see Fig. 1(b)]. The operator $\widehat{\boldsymbol{W}}_{\text{eff}}$, is nothing but somewhat arbitrary convention, valid as long as one get holds of all configuration functionals, such as potential-like energy terms from the original Hamiltonian operator, which are z-component momentum free.[12, 15] Then

$$\widehat{\boldsymbol{W}}_{\text{eff}} = \begin{pmatrix} W_{11} & W_{12} & 0 & 0 \\ W_{12}^{*} & W_{22} & 0 & 0 \\ 0 & 0 & W_{22} & W_{12} \\ 0 & 0 & W_{12}^{*} & W_{11} \end{pmatrix} \tag{8}$$

is suitable for going through a standard calculation

$$\left[\widehat{\boldsymbol{W}}_{\text{eff}} - V_{\text{eff}}\boldsymbol{I}_4\right]\boldsymbol{\Psi}(z) = \boldsymbol{O}_4, \tag{9}$$

leading us to the effective potential *band offset* V_{eff}, "*felt*" in some sense, by holes during their passage trough the heterostructure, as κ_{T} changes.

We introduced $W_{11(22)} = A_{1(2)}\kappa_{\text{T}}^2 + V(z)$ and $W_{12} = \frac{\hbar^2\sqrt{3}}{2\,m_0}\left(\gamma_2(k_y^2 - k_x^2) + 2i\gamma_3 k_x k_y\right)$, with γ_i the Lüttinger parameters, and m_0 the bare electron mass. The $\vec{\kappa}_{\text{T}}$ components $k_{x,y}$, are set in-plane respect to the heterostructure interfaces. In (9) $\boldsymbol{\Psi}(z)$ is a multi-component envelope function. Though moderately rough, assertion (8) represents a reliable-accuracy approximation to the V_{eff}, whose modifications we are interesting in. Let us consider a periodic three-layer [A-cladding left (L) layer /B middle (M) layer/ A-cladding right (R) layer] heterostructure, in the absence of external fields or strains.

In the bulk cladding layers, *hh* and *lh* modes mix due to the $\boldsymbol{k}\cdot\boldsymbol{p}$ interaction, while the middle slab represents a inhospitable medium for holes. At zero valence-band mixing, one has

$$\boldsymbol{V}(z)=\left\{\begin{array}{lll} 0 & ; & z<z_{\rm L} \\ V_{\rm B}-V_{\rm A}=V_{\rm eff} & ; & z_{\rm L}<z<z_{\rm R} \\ 0 & ; & z>z_{\rm R} \end{array}\right\}=\Theta V_{\rm eff}, \tag{10}$$

being Θ a step-like function, and $V_{\rm A/B}$ the potential of the cladding/middle layer. Due the lack of strict superlattice multiple-layered structures under study, we have neglected the spontaneous in-layer polarization field for III-nitride constituent media [21], thus assuming a rectangular potential profile as test-run input, rather than biased one for all envisioned III-nitride slabs of the heterostructures.

Strain field may rise questions on their relative effects on the electronic structure and, in particular on the valence-band structure where shape and size of the potential profile lead to stronger hybridization of the quantum states. Lets turn now to examine the effects of the stress, in the framework of the KL model Hamiltonian. The existence of a biaxial stress applied upon the plane parallel to the heterostructure interfaces, leads to the appearance of an in-plane strain. The effective potential operator $\widehat{\boldsymbol{W}}_{\rm eff}$ (8) in the presence of biaxial strain, can be written as [18]

$$\widehat{\widehat{\boldsymbol{W}}}_{\rm eff}=\widehat{\boldsymbol{W}}_{\rm eff}+U_s\boldsymbol{I}_4, \tag{11}$$

where

$$U_s=-\left\{a_v(2\varepsilon_1+\varepsilon_3)+b(\varepsilon_1-\varepsilon_3)\right\}, \tag{12}$$

is the accumulated strain energy resulting from the tensile or compressive stress acting on the crystal, when an epitaxial layer is grown on a different lattice-parameter substrate. Owing to strictness in formulation,[18] we guess that a maximum-quota criterium (12) it suffices to cover properly the aim posted in section 1. So, being independent from $\kappa_{\rm T}$, a maximized U_s was taken for granted, to evaluate if there is a real challenger strain effect respect to valence-band mixing influence on the metamorphosis of $V_{\rm eff}$. Here, the subscript s stands for strain. In (12) a_v/b represent the Pikus-Bir deformation/break potentials, describing the influence of hydrostatic/uniaxial strain. Meanwhile $\varepsilon_{1,3}$, are the in-plane, and normal-to-plane lattice displacements, respectively. For commonly used cubic and hexagonal semiconductor compounds, we assume[16, 17]

$$\varepsilon_1=-\frac{a_s-a_l}{a_l} \tag{13}$$

being $a_{s,l}$ the lattice parameter of the substrate and the epitaxial layer, respectively. Though no external stress is considered along the growth direction z, the lattice parameter is forced to change due to the Poisson effect.[17] Hence, the normal-to-plane displacement can be cast as

$$\varepsilon_3=-\nu\,\varepsilon_1, \tag{14}$$

which remains connected to in-plane deformation ε_1 via the Poisson radio ν. The last is valid for zinc blende and wurtzite materials.

By changing the material and the growth plane, the value of ν modifies. For cubic materials it reads[16]

$$\nu_{cub} = \begin{cases} 2\frac{C_{12}}{C_{11}} & \text{for growth plane: (001)} \\ \frac{C_{11}+3C_{12}-2C_{44}}{C_{11}+C_{12}+2C_{44}} & \text{for growth plane: (110)} \\ \frac{2(C_{11}+2C_{12}-2C_{44})}{C_{11}+2C_{12}+4C_{44}} & \text{for growth plane: (111)} \end{cases}, \tag{15}$$

while for the hexagonal ones we have[16]

$$\nu_{hex} = \begin{cases} 2\frac{C_{13}}{C_{33}} & \text{for growth plane: (0001)} \\ \frac{C_{12}\varepsilon_1+C_{13}\varepsilon_c}{C_{11}} & \text{for growth plane: } (1\bar{1}00) \\ \frac{C_{12}\varepsilon_1+C_{13}\varepsilon_c}{C_{11}} & \text{for growth plane: } (1\bar{1}02) \end{cases}. \tag{16}$$

To quote the parameter $\varepsilon_c = ((c_s - c_l)/c_l)$, we take c_s for the substrate wafer,[22] while c_l is referred to the epitaxially-grown layer on buffer stratum.

3. Discussion of results

Unless otherwise specified, the graphical simulations of V_{eff} reported here, were calculated using highly specialized $III-V$ semiconductor binary(ternary)-compound cases for both unstressed and stressed cubic and hexagonal systems. The present numerical simulations consider different constituent media, regardless if they can be grown. In this section, we briefly present numerical exercises within the *root-locus-like* technique, to foretell multiband-coupled charge-carrier effects for pseudomorphically stressed $III-V$ semiconductor layered systems.

3.1. Simulation of V_{eff} profile evolution

On general grounds, for $\kappa_{\text{T}} \approx 0$ the V_{eff} **is constant** [13, 15], while by letting grow κ_{T}, the band mixing effects arise and V_{eff} changes [12, 13, 15]. Some authors had declared a shift upward in energy, of the boundstates in the effective potential well as the transverse wave vector increases [14]. We are focused here to evaluate first the stress-free systems, and then the effect of a pseudomorphic strain on V_{eff}.

3.1.1. Unstressed V_{eff} metamorphosis To gain some insight into the rather complicated influence of the band mixing parameter κ_{T}, on the effective *band offset*, we display several graphics in the present section. The central point here, is a reliable numerical simulation for the spatial distribution of V_{eff} while the valence-band mixing increases from $\kappa_{\text{T}} \approx 0$ (uncoupled holes) to $\kappa_{\text{T}} = 0.1\text{Å}^{-1}$ (strong hole band mixing). This purpose requires

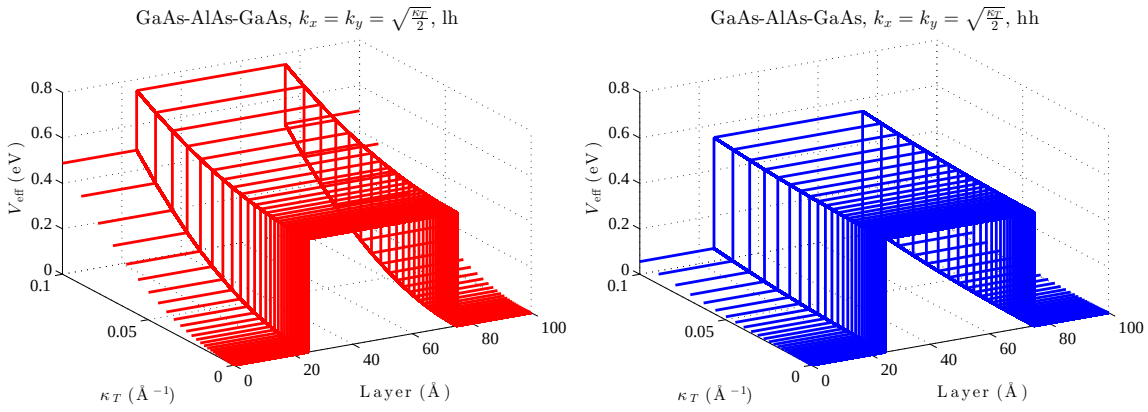

Figure 2. (Color online) Panel (a)/(b) displays the metamorphosis of the effective potential profile $V_{\rm eff}$ for *lh*/*hh* (red/blue lines), as a function of $\kappa_{\rm T}$ and layer dimension for a *GaAs*/*AlAs*/*GaAs* heterostructure.

a solution of (9) looking for a systematic start-point theoretical treatment of highly specialized $III-V$ semiconductor binary-compound cases of interest. We have set a width of 25 Å for the external cladding-layer L and R, while for the middle one we have taken a thickness of 50 Å.

Figure 2 demonstrates that the standard fixed-height rectangular distribution for V_z (10), is a consistent potential-energy trial of a QB for *hh* (blue lines), applicable in the wide range of $\kappa_{\rm T}$ [see panel (b)]. On the contrary, panel (a) remarks that the fixed-height QB is no longer valid for *lh* (red lines), as $\kappa_{\rm T}$ increases. Is in this very sense, when the valence-band mixing effects get rise, that become unavoidable to refer an effective *band offset* for a realistic description of the interplay of the envisioned physical structure with holes. We display in panel (a), the metamorphosis of $V_{\rm eff}$ for *lh*, as a function of $\kappa_{\rm T}$ and layer dimension for a *GaAs*/*AlAs*/*GaAs* heterostructure. Two changes are neatly observable, namely: the energy edge of both left and right cladding-layers steps up in almost 0.5 eV, while for the middle one it remains almost constant. The last departs from the $V_{\rm eff}$ evolution for *hh*, where all borders move up almost rigidly [see panel (b)]. Although not shown here owing to brevity, a similar behavior was found for other middle-layer alloys (*AlSb*, *AlP*, *AlN*). Described above features, remain under modification of the in-plane direction.

An appealing situation arises, at a specific entry of the transverse momentum. An earlier detailed study on this subject, [12] had predicted the existence of such quantity $\kappa^2_{\rm To} = 2V_o m^{\rm A} m^{\rm B}\left[\hbar^2\left(m^{\rm B}-m^{\rm A}\right)\right]$, for which $V_{\rm eff}$ becomes constant along the entire layered heterostructure. In the case envisioned here, due the presence of *hh* and *lh*, we have

$$\kappa^2_{{\rm To}(hh,lh)} = \frac{2V_o m_o^3\hbar^2}{\left(\gamma_1^{\rm A}\mp 2\gamma_2^{\rm A}\right)\left(\gamma_1^{\rm B}\mp 2\gamma_2^{\rm B}\right)}\left[\frac{1}{\left(\gamma_1^{\rm B}\mp 2\gamma_2^{\rm B}\right)}-\frac{1}{\left(\gamma_1^{\rm A}\mp 2\gamma_2^{\rm A}\right)}\right], \quad (17)$$

being $V_o = V_{\rm eff}(\kappa_{\rm T}=0)$, and A/B standing for cladding/middle layer. A direct

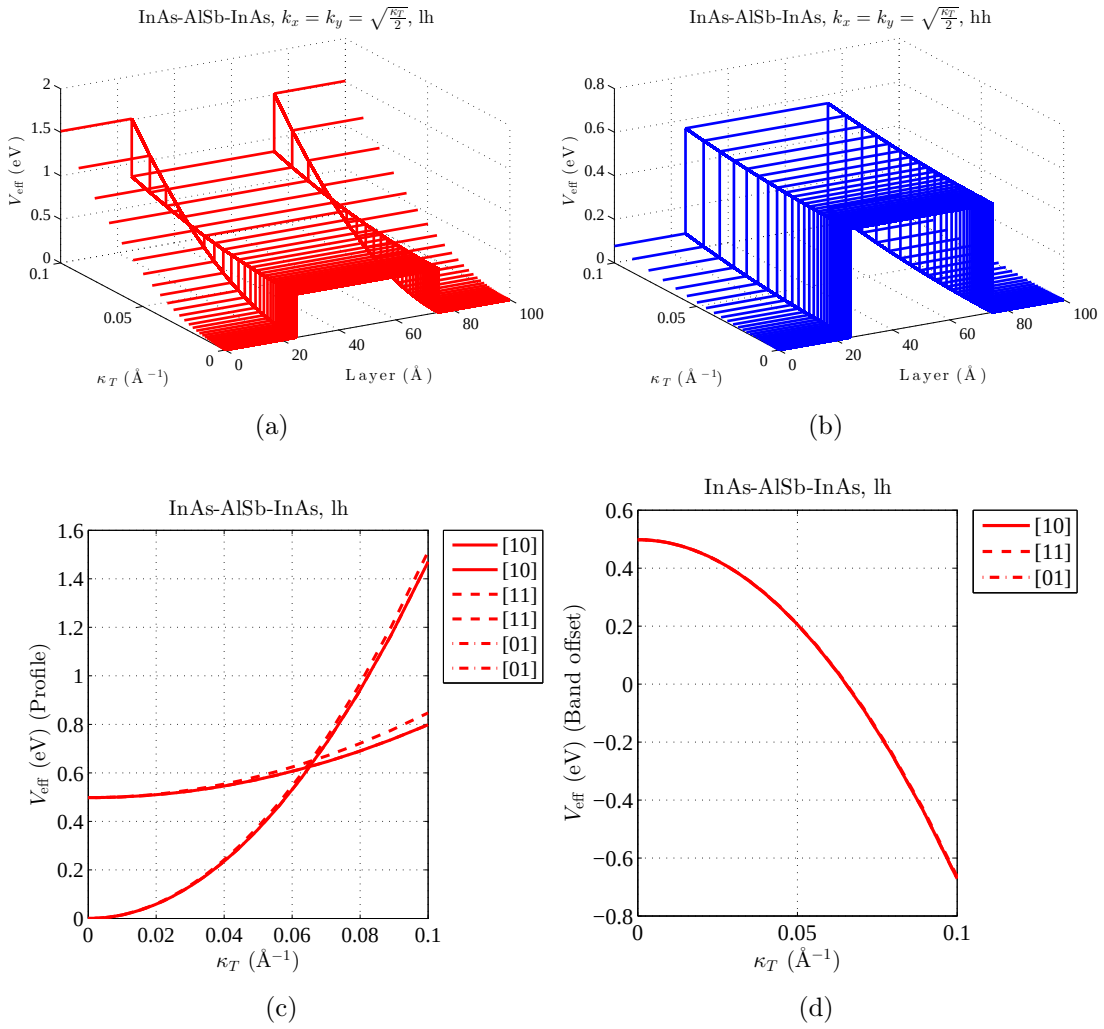

Figure 3. (Color online) Panel (a)/(b) displays the 3*D*-perspective evolution of the $V_{\rm eff}$ profile for *lh*/*hh* (red/blue lines), as $\kappa_{\rm T}$ and layer dimension grow. Panel (c) displays a cut of the $V_{\rm eff}$ profile for *lh* (red line), at the interface plane between left and middle layers, as a function of $\kappa_{\rm T}$. Panel (d) shows the progression of the *band offset*, at the same interface for *lh*, *i.e.* the difference between the upper-edge and lower-edge of the $V_{\rm eff}$ profile. We have considered a *InAs*/*AlSb*/*InAs* stress-free layered heterostructure.

consequence for $V_{\rm eff}$ being flat at $\kappa_{\rm To}$, is the existence of a crossover of $V_{\rm eff}$ respect to (17). In other words, if a QW-like profile is present for $\kappa^2_{{\rm T}(hh,lh)} < \kappa^2_{{\rm To}(hh,lh)}$, then a QB-like profile appears at $\kappa^2_{{\rm T}(hh,lh)} > \kappa^2_{{\rm To}(hh,lh)}$, or the other way around.

In Figure 3(a) the $V_{\rm eff}$ valence-band mixing dependence, exhibits a neatly permutation of the $V_{\rm eff}$ character as the one predicted for electrons [12]. This permutation pattern is what we call as "*keyboard*" effect, and was detected for *lh* only in stress-free systems. This strike interchange of roles for QB-like and QW-like layers, whenever the in-plane kinetic energy, varies from low to large intensity, represents the most striking contribution of the present study. For a single-band-

electron Schrödinger problem, some authors had predicted that both QW and QB may appears in the embedded layers of a semiconductor superlattice, depending on the transverse-component value of the wave vector.[12] Recently had been unambiguously demonstrated, that the effective-*band offset* energy $V_{\rm eff}$, "*felt*" by the two flavors of holes, as $\kappa_{\rm T}$ grows, is not the same. Inspired on these earlier results, we had addressed a wider analysis of this appealing topic, displayed in Figure 3, pursuing a more detailed insight. We have considered a *InAs*/*AlSb*/*InAs* heterostructure. Panel (a)/(b) of Figure 3 shows explicitly the metamorphosis of $V_{\rm eff}$, felt for both flavors of holes independently, respect to concomitant-material slabs. From panels (a) and (b), it is straightforward to see, that for *hh* (blue lines), an almost constant $V_{\rm eff}$ remains, while $\kappa_{\rm T}$ varies from 0 (uncoupled holes) to 0.1Å^{-1} (strong hole band mixing), despite the respective band-edge levels had changed. At variance with the opposite for *hh* [blue lines, panel (b)], the *lh* exclusively [red lines, panel (a)] exhibit the *keyboard* effect, *i. e.* they feel an effective *band offset* exchanging from a QW-like into a QB-like one, and viceversa for an *InAs*/*AlSb*/*InAs* heterostructure, while $\kappa_{\rm T}$ increases. The evident *keyboard* effect of $V_{\rm eff}$, resembles a former prediction for electrons [12]. This observation means, that in the selected rank of parameters for a given binary-compound materials, a *lh* might "*felt*" a qualitative different $V_{\rm eff}$ (QW or QB), during its passage through a layered system, while it is varying the degree of freedom in the transverse plane. Former assertions can be readily observed in Figure 3(c)-(d), were we had plotted the evolution of $V_{\rm eff}$ profile [panel (c)], as well as the progression of the *band offset* [panel (d)], with $\kappa_{\rm T}$ at a fixed transverse plane of the heterostructure. Both upper-edge and lower-edge move in opposite directions [see panel (c)] and the zero-*band offset* point configuration is detected in the vicinity of $\kappa_{\rm T} \approx 0.066\text{Å}^{-1}$ [see panel (d)]. The permutation holds for other in-plane directions, as can be seen from panel (c). Although not shown here for simplicity, the *keyboard* effect, remains robust for other middle-layer binary compounds, namely: *AlAs*, *AlP*, and *AlN*.

3.1.2. Keyboard effect `versus` *pseudomorphic strain.* Turning now to built-in elastic stressed layered heterostructures, we are interested to answer a simple question: wether or not the existence of a pseudomorphic strain becomes a weak or a strong competitor mechanism, able sometimes just to diminish the *keyboard* effect on $V_{\rm eff}$, or even make it rises/vanishes occasionally. Thereby, we need to account the accumulated strain energy resulting from the tensile or compressive stress acting on the crystal slabs. The last requires to solve (11), presuming the heterostructure sandwiched into a pseudomorphically strained QW/QB/QW-sequence.

Figure 4 is devoted to demonstrate that the *keyboard* pattern for *lh* remains robust in a *InSb*:*InSb*/*AlN*/*InSb* pseudomorphically strained layered heterostructure [see panel (b)], respect to that of the stress-free system [see panel (a)]. In this case, we conclude that maximized U_s (12) do not represent any antagonist mechanism regarding to valence-band mixing influence on $V_{\rm eff}$.

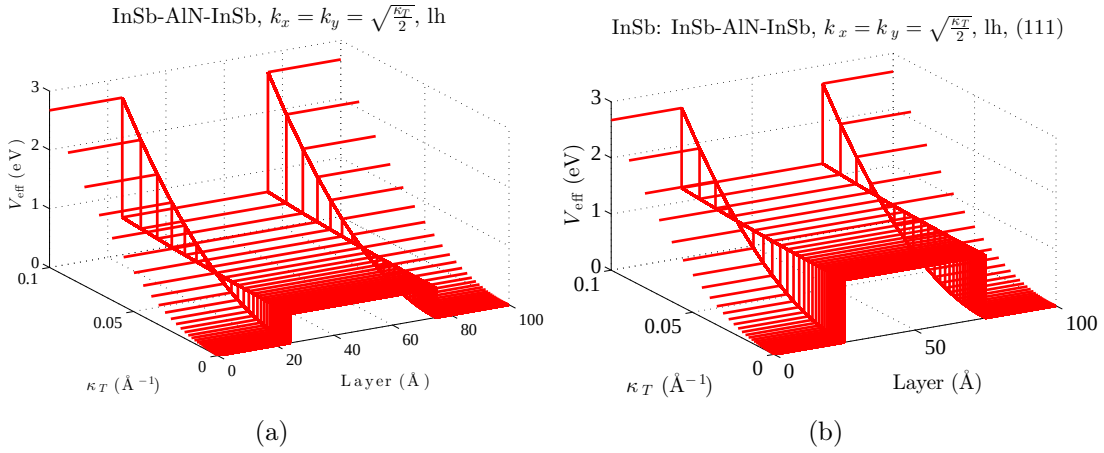

Figure 4. (Color online) Panel (a) displays the $3D$-perspective evolution of the stress-free $V_{\rm eff}$ profile for *lh* as $\kappa_{\rm T}$ and layer dimension grow. Panel (b) shows the same for a *InSb*:*InSb*/*AlN*/*InSb* strained layered heterostructure.

3.2. Influence of the pseudomorphic strain on k_z-spectrum

The QEP k_z-spectrum is a meaningful, and well-founded physical quantity that can be obtained *via* the *root-locus-like* procedure [19] by unfolding back in the complex plane the dispersion-curve values for bulk materials, determined by stress-induced effects on the stress-free heterostructure. Thus, we take advantage of the *root-locus-like* know-how, to promptly identify evanescent modes, keeping in mind that complex (or pure imaginary) solutions are forbidden for some layers and represent unstable solutions underlining the lack of hospitality of these slabs for oscillating modes. The opposite examination is straightforward and also suitable for propagating modes, which become equated with stable solutions for given layers.

To obtain the QEP k_z-spectrum in a periodic pseudomorphically strained heterostructures of QB-acting/QW-acting/QB-acting materials, we first use (11) and substitute it in (8). Next, we solve again the characteristic problem (9), whose eigenvalues allow us to obtain the new expression for the QEP-matrix $\boldsymbol{\mathcal{K}}$, and then finally consequently solve (2) for k_z. Once we have quoted the eigenvalues k_z of (7), it is then straightforward to generate a plot in the complex plane, symbolizing the locations of k_z values that rise as a band mixing parameter $\kappa_{\rm T}$ changes. Keeping in mind that complex (or pure imaginary)/real solutions of (7) represent forbidden/allowed modes, we take advantage of the *root-locus-like* map to identify evanescent/propagating modes for a given layer. Thus, we are able "to stamp" on a $2D$-map language, a frequency-domain analysis of the envisioned heterostructure under a quantum-transport problem. This way, we are presenting an unfamiliar methodology in the context of quantum solid state physics, to deal with low-dimensional physical phenomenology.

The Figure 5 and Figure 6, illustrate the role of band mixing for $\kappa_{\rm T}\,[10^{-6}, 10^{-1}]$ Å^{-1}, on the k_z spectrum from QEP (7), for a $III-V$ strained alloy, clearly distinguished as QW in most layered systems with technological interest. Importantly, by assuming two

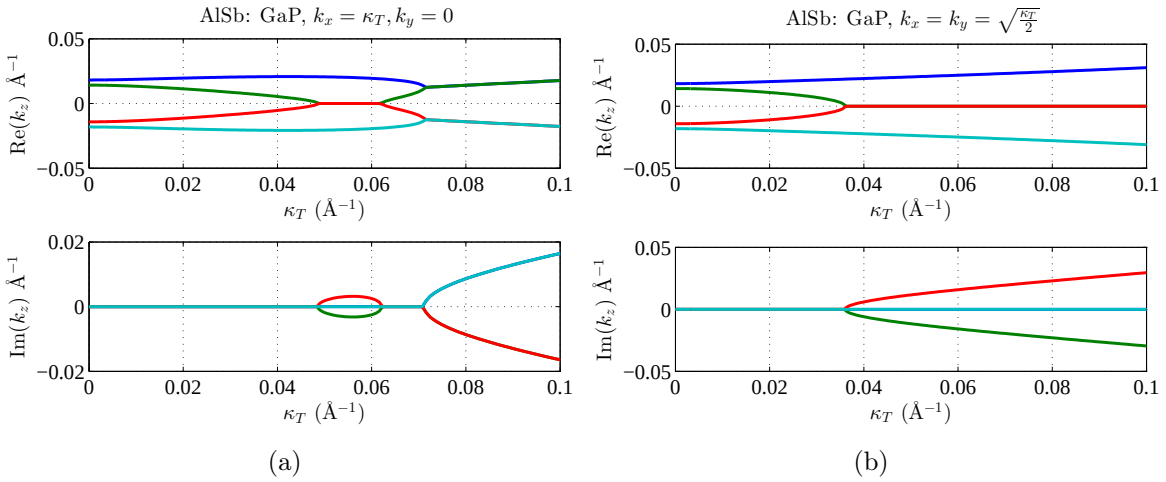

Figure 5. (Color online) Root locus for the eigenvalues k_z from QEP (7), as a function of $\kappa_{\rm T}$ for strained *AlSb*(substrate)/*GaP* (epitaxial layer). We had assumed $E = 0.6$ eV, and in-plane directions [10]/[01] for panel (a)/(b).

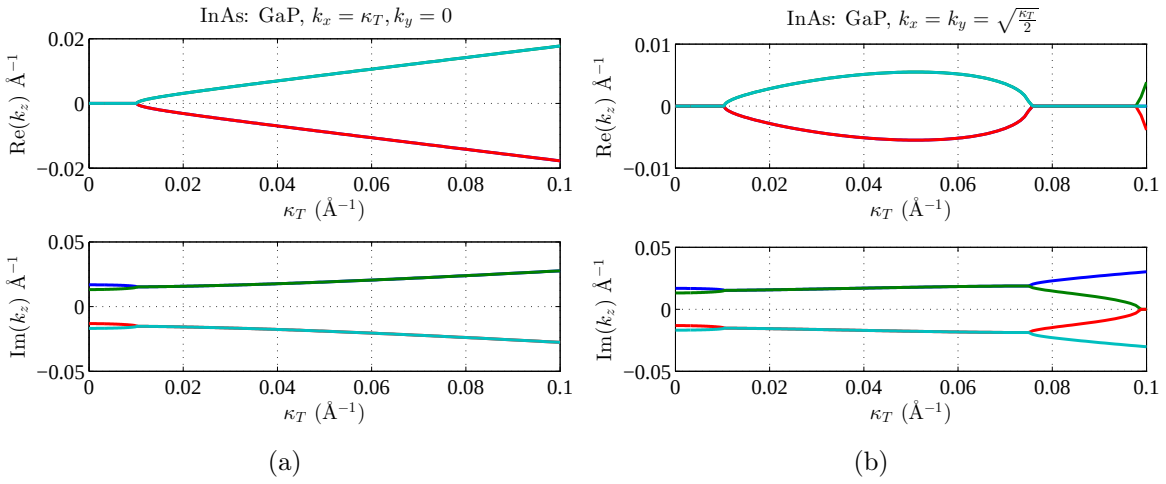

Figure 6. (Color online) Root locus for the eigenvalues k_z from QEP (7), as a function of $\kappa_{\rm T}$ for strained *InAs*(substrate)/*GaP* (epitaxial layer). We had assumed $E = 0.45$ eV, , and in-plane directions [10]/[01] for panel (a)/(b).

different substrates *AlSb* (Fig.5) and *InAs* (Fig.6), we found different patterns of the k_z spectrum for *lh* and *hh*. Namely for the [10] in-plane direction, the k_z *root-locus-like* evolution is real for *lh*, in the range of $\kappa_{\rm T} \in [10^{-6}, 0.049]$ Å^{-1} and $\kappa_{\rm T} \in [0623, 0.0708]$ Å^{-1}, while in the intervals $\kappa_{\rm T} \in [0.049, 0.0623]$ Å^{-1} and $\kappa_{\rm T} \in [0.0708, 0.1]$ Å^{-1}, k_z becomes pure imaginary and complex, respectively [see Fig.5(a), inner green-red solid lines]. On the other hand, the k_z *root-locus-like* shows real values for *hh*, in the interval $\kappa_{\rm T} \in [10^{-6}, 0.0708]$ Å^{-1} and is complex, when $\kappa_{\rm T} \in [0.0708, 0.1]$ Å^{-1} [see Fig.5(a) outer blue solid lines]. Worthwhile stress that *hh* and *lh* curves, are undistinguishable in this last interval. Although not shown here, the [01] in-plane direction exhibits the same behavior. The Fig.5(b), displays the QEP (7 spectrum along the [11] in-plane

direction. For lh only, k_z *root-locus-like* evolution starts as a real number in the range $\kappa_{\mathrm{T}} \in [10^{-6}, 0.0363]$ Å^{-1}, and becomes pure imaginary for $\kappa_{\mathrm{T}} \in [0.0363, 0.1]$ Å^{-1}. The k_z spectrum for hh it is always a real number in the whole selected interval $\kappa_{\mathrm{T}} \in [10^{-6}, 0.1]$ Å^{-1}. Panel (a) of Fig.6 describes in-plane direction [10], and for analogy the [01] – although not depicted for brevity–, with the band mixing. For both lh and hh, the k_z evolution starts as a pure imaginary number in the range $\kappa_{\mathrm{T}} \in [10^{-6}, 0.01]$ Å^{-1}, and become a complex number in the interval $\kappa_{\mathrm{T}} \in [0.01, 0.1]$ Å^{-1}. In this gap the hh and lh are indistinguishable, as their k_z magnitude is the same. Meanwhile, the panel (b) of Fig.6 demonstrates that for the [11] in-plane direction, the k_z values are mostly complex or pure imaginary, except in the small interval of $\kappa_{\mathrm{T}} \in [0.097, 0.1]$ Å^{-1}, where they are real. None real entries of k_z for hh, were found as κ_{T} changes within the bounds $[0.01, 0.1]$ Å^{-1}. The hh and lh curves are indistinguishable in the range of $\kappa_{\mathrm{T}} \in [0.0133, 0.075]$ Å^{-1}. After this detailed description, several features deserve close attention. In short: the [10] and [01] in-plane directions, show an isotropic behavior, for each selected substrate. The real-value domains of the *root-locus-like* map of k_z, means that the GaP strained-layer recovers his standard QW-behavior for both hh and lh quasi-particles, regarding the stress-free configuration. On the opposite, whenever real-value map fades, *i.e.* complex or pure imaginary magnitudes arise, none oscillating modes can propagate through an $InAs : GaP$ strained slabs. In this last case, the GaP might turns into an effective QB, for traveling holes.

4. Conclusions

We present an alternative procedure to simulate graphically, the phenomenon of the transverse degree of freedom influence on the effective scattering potential. For low-intensity valence-band mixing regime, a fixed-height rectangular distribution of the potential-energy, is a good trial as a standard reference frame, for a theoretical treatment involving both flavors of holes under study. However this assertion is no longer valid, whenever the mixing effects reveal. At variance with the opposite for hh, the lh exclusively, experience the strike *keyboard* effect and permutations of V_{eff} in stress-free systems. Our results provide an unambiguous demonstration for the apparent robustness of the fixed-height flat V_{eff} as test run input whenever pure hh and lh, are mixed. Pseudomorphic strain is able to diminish the *keyboard* effect on V_{eff}, and also makes it emerge or even vanish eventually. We conclude that the multiband-mixing effects modulated by stress induced events, are competitors mechanisms that can not be universally neglected by assuming a fixed-height rectangular spatial distribution for fixed-character potential energy, as a reliable test-run input for semiconducting heterostructures. Present modelling of V_{eff} evolution, may be a reliable workbench for testing other configurations, besides our results may be of relevance for promising heterostructure's design guided by valence-band structure modeling to enhance the hole mobility in III-V semiconducting materials provided they always lagged compared to II-IV media [8].

Acknowledgments

This work was developed under support of DINV, UIA, México. One of the authors (L.D-C) is grateful to the Visiting Academic Program of the UIA, México.

References

[1] G. Klicmeck, R. Ch. Bowen, and T. B. Boykin, Superlattices and Microstructures **29**, 187 (2001).
[2] R. Wessel and M. Altarelli, Phys. Rev. B 39, 12802 (1989).
[3] H. Schneider, H. T. Grahn, K. Klitzing, and K. Ploog, Phys. Rev. B **40**, 10040 (1982).
[4] A. C. Bittencourt, A. M. Cohen and G. E. Marques, *Brazilian J. Phys.* **27**, 281 (1997).
[5] Bradley A. Foreman, *Phys. Rev. B* **76**, 045327 (2007)
[6] N. J. Ekins-Daukes, K. W. J. Barnham, J. P. Connolly, J. S. Roberts, J. C. Clark, G. Hill and M. Mazzer, *App. Phys. Lett.* **75**, 4195 (1999).
[7] T. M. Smeeton, M. J. Kappers, J. S. Barnard, M. E. Vickers and C. J. Humphreys, *App. Phys. Lett.* **83**, 5419 (2003).
[8] Aneesh Nainani, Brian R. Bennett, J. Brad Boos, Mario G. Ancona and Krishna C. Saraswat, arxiv.org/pdf/1108.5507 (2011).
[9] D. A. Faux, J. R. Downes and E. P. OReilly, *J. App. Phys.* **82**, 3754 (1997).
[10] Sunil Patil, W. P. Hong and S. H. Park, *Phys. Lett. A* **372**, 4076 (2008).
[11] Manish K. Bashna, Pratima Sen and P. K. Sen, *Indian J. Pure App. Phys.* **51**, 553 (2013).
[12] V. Milanovic, and D. Tjapkin, *Phys. Stat. Sol(b)* **110**, 687 (1982).
[13] Rolando Pérez-Álvarez and Federico García-Moliner,"*Transfer Matrix, Green Function and related techniques:Tools for the study of multilayer heterostructures*", (Ed. Universitat Jaume I, Castellón de la Plana, España), 2004.
[14] S. Ekbote, M. Cahay and K. Roenker, *J. App. Phys.* **85**, 924 (1999).
[15] L. Diago-Cisneros, H. Rodríguez-Coppola, R. Pérez-Álvarez, and P. Pereyra, *Phys. Rev. B* **74**, 045308 (2006).
[16] K. H. Yoo, J. D. Albrecht and L. R. Ram-Mohan, *Am. J. Phys.*, **78**, 589 (2010).
[17] V. D. Jovanović, "*Quantum Wells, Wires and Dots*", (Ed. John Wiley & Sons, Ltd.), 2005.
[18] Joachim Piprek, "*Semiconductor Optoelectronic Devices. Introduction to Physics and simulation*", (Ed. Elesevier, Acadenic Press), 2003.
[19] A. Mendoza-Álvarez, J. J. Flores-Godoy, G. Fernández-Anaya, and L. Diago-Cisneros, *Phys. Scr.* **84**, 055702 (2011).
[20] J. J. Flores-Godoy, A. Mendoza-Álvarez, L. Diago-Cisneros, and G. Fernández-Anaya *Phys. Status Slidi B*, **67**, 1339 (2113).
[21] O. Ambacher, J. Majewski, C. Miskys, A. Link, M. Hermann, M. Eickhoff, M. Stutzmann, F. Bernardini, V. Fiorentini, V. Tilak, B. Schaff, and L. F. Eastman, *J. Phys.: Condens. Matter* **14**, 3399 (2002).
[22] I. Vurgaffman, J. R. Mayer, and L. R. Ram-Moham, *J. App. Phys.* **89**, 5815 (2001).